Indian Journal of Chemical Technology
Vol. 27, March 2020, pp. 116-125

Adsorption equilibrium, isotherm, kinetics, and thermodynamic of modified bentonite for removing Rhodamine B

Yuzhen Li*[,1], Zhihui Huang[1], Yunsheng Xia[2], Jianhui Shi[1] & Lizhen Gao[1,3]
[1]College of Environmental Science and Engineering,
[1]Taiyuan University of Technology, 79 Yingze Street, Yingze District, Taiyuan, 030024, China
[2]College of Chemistry and Chemical Engineering, Bohai University, Jinzhou, 121013, China
[3]School of Mechanical Engineering, University of Western Australia, 35 Stirling Highway, WA 6009, Australia
E-mail: liyuzhen123456@126 com

Received 1 December 2018; accepted 30 January 2020

Anionic and cationic surfactant modified sodium bentonite (Na-Bt) has been prepared by the cationic surfactant cetyltrimethyl ammonium bromide (CTAB) and the anionic surfactant sodium dodecyl benzene sulfonate (SDBS) to sodium bentonite, respectively. The properties of the modified samples are characterized by XRD, SEM, BET and FT-IR. The results of characterization shown that the cationic surfactant had changed the structure and properties of natural sodium bentonite, which proved that surfactants had been successfully implanted into sodium bentonite. But anionic surfactant had no change, this manifested SDBS didn't insert the layers of bentonite. In addition, adsorption experiments of Rhodamine B (RhB) proved that the modified sodium bentonite adsorption performance is greatly improved. The adsorption experiments also indicated that CTAB-bentonite had the largest adsorption capacity compared with SDBS-bentonite due to the formation of a highly effective partition medium by cationic surfactant micelle. The adsorption data of RhB is analyzed with the isothermal model, thermodynamics and kinetics. Overall, this study provided high-efficiency method for the removal RhB by the surfactant modified bentonite.

Keywords: Na-bentonite, Surfactant modification, Adsorption, Rhodamine B

Currently, the state's laws and regulations of poisonous and harmful emissions were more and more strict. Printing and dyeing industries were known to generate high volumes of wastewaters, in which the main pollutant was the dye. A variety of dyes were toxic and not easy to be degraded. In order to decrease the amount and toxicity of the dye wastewaters, many researchers have been dedicated to augmenting the degree of immobilization of the dyes onto the fibres[1-5]. Furthermore, dyeing groups caused serious destruction for the water environment, which was reported to generate carcinogens to fatally harm human health and could lead to negative influence to the environment and ecosystem as well[6-8]. Therefore, Studying out the better solution is facing one of the enormities of the task for all researchers.

Many technologies have been applied to purify the dyeing wastewater including chemical method, adsorption, electrochemical oxidation, membrane separation and so on[9]. Currently, in the field of water treatment, appearing numerous methods, such as oxidation methods, biological methods, etc. Oxidation methods can be divided into advanced oxidation and chemical oxidation processes, they have been shown to be operative in degrading a variety of dyes. However, the major disadvantage of using oxidation methods were that it may produce some toxic byproducts even from biodegradable dyes in wastewater, which was not beneficial to thoroughly remove pollutants[10,11]. In recent years, biological treatment of dyes wastewater has been investigated by many researchers for influencing factors The results indicated that the efficiency of removal dyes were good and did not produce secondary pollution, but the biological methods remove only the dissolved dyes and were strict with environment conditions[12-14].

In many ways of treating dyes, adsorption method was relatively common and effective. The development of adsorbent was particularly important. One of the bentonite as adsorbent had more advantages. The main component of bentonite is the non-metallic minerals of montmorillonite, and the properties, chemical composition and the internal structure of the bentonite were closely related with adsorption performance. The internal 2:1 type of crystal structure of montmorillonite was made up of

two silicon oxygen tetrahedron clipping a layer of alumina octahedral, which the chemical formula was $Al_3O_2 \cdot 4SiO_2 \cdot 3H_2O$[15] Interlayer domains of bentonite have many special properties, such as cationic exchange, macromolecule polymerization, photocatalytic properties, interlayer column brace and adsorption, etc[16]. Therefore, bentonite has a broad development space for the field of water treatment.

Adsorption capacity of natural bentonite was the smaller and its surface shown hydrophilicity, therefore, it was poorer for adsorbing the organic matter. In practical application, people modified bentonite depending on the purpose. At present, the modified method of bentonite mainly included inorganic modification (thermal activation treatment, acid/alkali modification and pillared interlayer of metal, etc), The organic modification (the surfactant modification, the crosslinking agent modification and organic ligand inserted layer, etc) and inorganic/organic composite modification (the above-mentioned inorganic modification method and organic modification method of joint action)[17]. Manjot Toor *et al*. used three methods of activation of modified bentonite, the results shown that the thermal activation and acid activated bentonite surface area increased by 20 and 65% respectively, the acid activation combined with thermal activation treatment bentonite, which made its surface area increased by 70%, and three kinds of modified methods were improved bentonite adsorption ability of organic pollutants[18]. E Orucoglu *et al*. utilized the hexadecyl pyridine modified bentonite and used X-ray diffraction (XRD) analysis of expansion and thermal stability, explaining hexadecyl pyridine modified bentonite had good thermal stability and pure processing in favor of pollutants[19]. M Kotal *et al*. have prepared organic-inorganic composite modified bentonite and been used for adsorption of dye wastewater, the results shown that the treatment effect of compound of modified bentonite was better[20].

In the present study, the natural Na-bentonite has been modified by the cationic surfactant cetyltrimethyl ammonium bromide (CTAB) and the anionic surfactant sodium dodecyl benzene sulfonate (SDBS) to apply to adsorb Rhodamine B (RhB) from aqueous solution. For exploring the structural and properties of modified bentonite, the paper characterized its performance through a series of characterization methods (XRD, SEM, N_2 adsorption-desorption and FT-IR), which provided theoretical support for the research of adsorption performance. In order to study the effects of several factors, a series of experiments were carried out, selecting adsorbent dosage, contact time, initial dyes concentration, temperature and initial solution *p*H as the experimental variables for the adsorption of RhB onto modified bentonite and nature Na-bentonite. In addition, the adsorption kinetics, adsorption isotherms and thermodynamic studies were also detailed analyzed for adsorption of RhB onto modified bentonite.

Experimental Section

Materials

RhB (Molecular formula: $C_{28}H_{31}ClN_2O_3$) was acquired from Aladdin Chemistry Co., Ltd. (Shanghai, China), the structure of RhB was shown in Fig 1, and was supplied in the commercial form, with no purification. The aqueous solutions of RhB (concentration from 50 to 350 mg/L) were prepared, by dissolving the required mass of dye in distilled water. And its *p*H was adjusted by HCl of 0.1 mol/L or NaOH of 0.1 mol/L solutions. The Na-bentonite used in this study obtained from Heng Sheng material co., LTD (Henan ,China). The natural Na-bentonite contains 63.43 % SiO_2, 3.05 % MgO, 17.88 % Al_2O_3, 0.9 % K_2O, 2.22 % CaO, 2.06 % Fe_2O_3, 0.98 % Na_2O, 0.13 % TiO_2 and 8.09 % loss of ignition. The cation exchange capacity (CEC) of Na-bentonite was determined as 1.092 mmol/g by the barium clay method. The surfactant CTAB was purchased from Chemical reagent co., LTD (Shanghai, China). The surfactant SDBS was acquired from recovery of fine

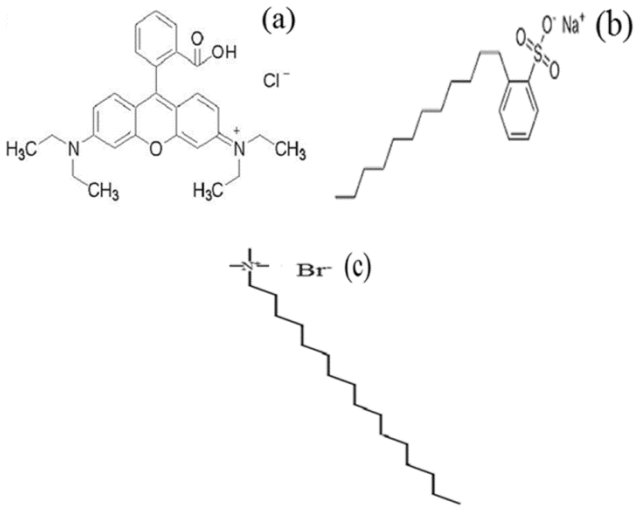

Fig. 1 — The molecular structure of (a) Rhodamine B, (b) SDBS and (c) CTAB.

chemical industry research institute (Tianjin, China). The molecular structure of CTAB and SDBS was displayed in Fig 1 All reagents were analytical grade Deionized water was used in all experiment.

The preparation of modified bentonite

The organic bentonites were synthesized by anionic/cationic surfactants implanted into Na-bentonite. The surfactants included SDBS and CTAB were used. The dosage of SDBS was equivalent to 100% of the CEC of Na-bentonite were dissolved in 1 L of distilled water and stirred for 3 h at 60°C. 10 g Na-bentonite was added to the above solution, and sequentially stirred for 3 h at 60°C. Then, the sample was pumped about separation and washed with distilled water several times, until the supernatant solution was free of bromide ions. The results were oven-dried at 80°C until the water was completely evaporated The product which was noted as SDBS-bentonite was ground into powder. In the same dosing quantity, the preparation conditions and methods, CTAB modified bentonite was prepared and was marked as CTAB-bentonite.

Adsorption experiments

Firstly, to study the adsorption performance of modified bentonite, effect of dosage of CTAB-bentonite and SDBS-bentonite were analyzed, selecting adsorbent additive quantity range was 0.04 g to 1.0 g Secondly, in order to determine the adsorption equilibrium time, each batch was conducted at various time intervals (10, 20, 30, 40, 50, 60, 70, 80, 90, 100, 110, 120, and 130) min. And adsorption studies were done by the optimum value of CTAB-bentonite and SDBS-bentonite with 50 mL of various dye solutions (50-350 mg/L) in a stoppered bottle and they were placed in a temperature controlled water bath shaker Finally, the *p*H of solutions was adjusted to the range from 2.0 to 10.0 by small amount of NaOH/HCl solution. In the process of adsorption experiment, the condition of the centrifugal separation was at the rotate speed of 3000 r/min for 15 min with low speed centrifuge. The remaining concentrations of each solution were measured by visible spectrophotometer at 554 nm (the λ_{max} value for RhB). The absorbance concentration profile was obtained by plotting the calibration curve between absorbance and dye concentration. The amount adsorbed of dye onto modified bentonite (q_e) can be estimated from formula:

$$q_e = \frac{(C_0 - C_e) \times V}{m} \times 100 \quad \ldots (1)$$

where q_e is the amount of dye adsorbed per unit mass of adsorbent (mg/L), C_0 and C_e (mg/L) are initial and equilibrium dyes concentration, V (L) is the volume of dyes solution, and m (g) is the adsorbent mass.

The removal efficiency of dye onto modified bentonite at time t was calculated by

$$\text{Removal efficiency (\%)} = \frac{C_0 - C_t}{C_0} \times 100 \quad \ldots (2)$$

where C_t (mg/L) is time t dyes concentration

Characterization of organoclay

The structure properties and surface morphology of CTAB-bentonite and SDBS-bentonite were characterized by XRD, SEM, N_2 adsorption-desorption and FT-IR. XRD was used to analyze the distance layers of the modified Na-bentonite with a Shimadzu XRD-6000 at a scanning rate of 2°/min in 2 θ ranging from 0.6°–70° with CuKa radiation (λ=0.154 nm), and advance diffract to meter operating at the voltage of 40 kV and a 30 mA flux. The d_{001} of the examined samples were calculated by Bragg's formula $2d\sin\theta=n\lambda$. The surface morphology of Na-bentonite and modified bentonite was confirmed under 10 KV voltage and a 5 mA flux with S4800 type of scanning electron microscopy (SEM). The adsorption-desorption isotherm of modified bentonite were finished by BET-analyzer (Kang Ta N22-27E) after degassing under vacuum at 80°C for 3 h. The specific surface area, the pore size and pore size of bentonite were obtained by the BET method. The total pore volume was calculated from the maximum amount of N_2 desorption at partial pressure (P/P_0) =0.95. FT-IR spectra study were realized by Bruker Tensor 27 spectrophotometer with KBr pellet technique and recorded in the range of 4000–400 cm^{-1}.

Results and Discussion

Characterization of the samples

XRD analysis

Figure 2 displayed the XRD patterns of three kinds of absorbents. In Fig. 2a, the interlamellar spacing of Na-bentonite was 1.50 nm (d_{001}) in 2θ = 5.87º, which represented the typical XRD pattern of Na-bentonite. After SDBS and CTAB inserted into Na-bentonite, the d_{001} peak in SDBS-bentonite changed to 7.06º (see Fig. 2b) and CTAB-bentonite shifted to 4.54º (see Fig. 2c), the corresponding interlayer spacing of SDBS-bentonite (d_{001}) and CTAB-bentonite (d_{001}) turned into 1.25 nm and 2.04 nm, respectively. This shown that CTAB had been inserted into the layer of

Na-bentonite by ion exchange, but SDBS failed to insert into the layer of Na-bentonite. For CTAB-bentonite, the change of the spacing layer shown that it was conducive to the adsorption process of RhB, which was attributed to the alkyl chain length of CTAB[21]. However, outside the plane of bentonite were negatively charged and generated electrostatic repulsion with anionic surfactant (SDBS), which led to SDBS could not enter to Na-bentonite interlayer and the layer spacing of Na-bentonite reduced[22]. The results indicated that cationic surfactant (CTAB) modified bentonite was more favorable for adsorption RhB.

SEM analysis

The SEM images of three materials revealed significant changes on the surface morphology of surfactant modification in Fig. 3. The SEM image of Na-bentonite displayed a smooth and irregular appearance, and natural Na-bentonite presented the scattered and different sizes of block structure (From Fig. 3a) In Fig. 3c, the SEM image of SDBS-bentonite had no big difference with Na-bentonite, it also formed different size of block structure and scattered, but the surface of SDBS-bentonite was slightly rough. However, the surface morphology of CTAB-bentonite was rough and accompanied by a small number of holes (see Fig. 3b), which was due to insert into Na-bentonite by CTAB. In addition, the SEM images of CTAB-bentonite shown the edge of the crimp morphology and formed a larger block than Na-bentonite.

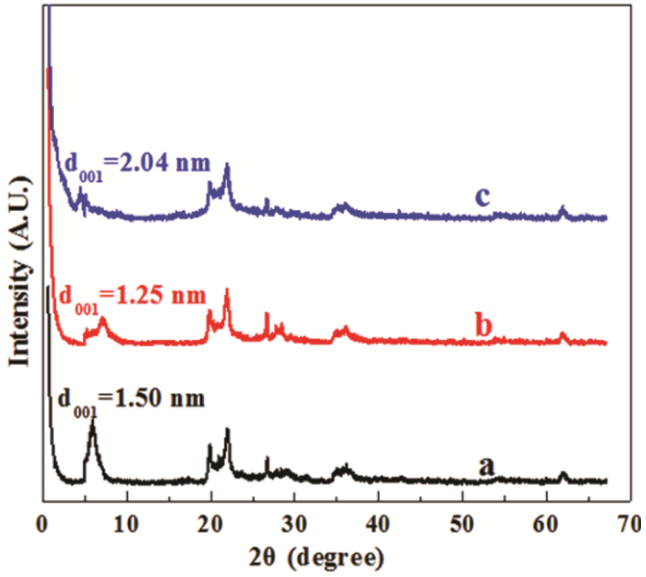

Fig. 2 — XRD patterns of samples. (a) Na-bentonite, (b) SDBS-bentonite, (c) CTAB-bentonite

N_2 gas adsorption-desorption analysis

The N_2 adsorption-desorption isotherms and pore size distribution of Na-bentonite and modified bentonite were shown in Figure 4. From Fig. 4, with relative pressure $0.44<P/P_0<0.97$, adsorption-desorption isotherms of three materials began to slowly ascend, but adsorption/desorption isotherms didn't maintain overlap and appeared the obvious lag phenomenon of regression. Hysteresis loop belonged to typical H_3. The reasons for this phenomenon was no obvious adsorption limit for flake particle materials (such as clay), or seam hole materials in the region of the high relative pressure[23].

Table 1 summarized BET analysis results of samples. In Table 1, it can reveal that specific surface area, pore volume and pore size of the CTAB-bentonite (32.735 m^2/g, 0.078 cm^3/g, 3.865 nm) was lower than Na-bentonite (74.351 m^2/g, 0.137 cm^3/g, 3.866 nm), respectively. Indicating that CTAB had entered into the interlayer of bentonite and blocked the channel between the layers, reducing the surface area, pore volume and pore size. But specific surface area and pore volume of SDBS-bentonite were 81.680 m^2/g and 0.179 cm^3/g, respectively, which were higher than Na-bentonite. The pore size of SDBS-bentonite was 3.832 nm, the value was slightly lower

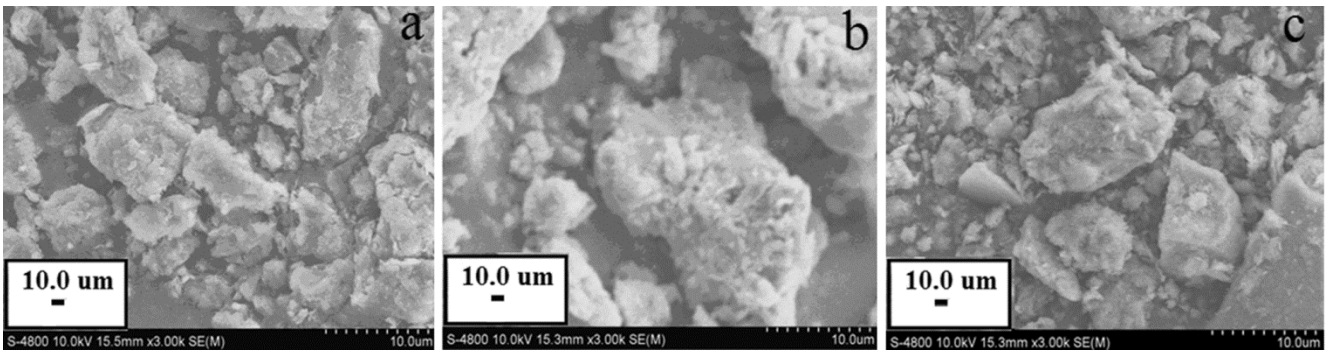

Fig. 3 — SEM images of samples (a) Na-bentoniteand, (b) CTAB-bentonite and (c) SDBS-bentonite

than Na-bentonite. This was because of the SDBS adhered on the surface of the bentonite. The result led to block the hole of bentonite and be enlarged for pore volume and slightly decrease for the aperture.

FT-IR analysis

Figure 5 shown the FT-IR spectra (4000-400 cm^{-1}) of (a) Na-bentonite, (b) SDBS-bentonite, and (c) CTAB-bentonite. The FT-IR spectra of the modified bentonite and Na-bentonite had roughly the same peak shape, which indicated that the basic skeleton of Na-bentonite had no obvious change in the process of modification. In the wavenumber of 810 cm^{-1}, the FT-IR spectra of Na-bentonite, SDBS-bentonite and CTAB-bentonite appeared Al-O stretching vibration peak; in 1041 cm^{-1}, Na-bentonite and two kinds of modified bentonite formed Si-O stretching vibration absorption peak; in 3417 cm^{-1}, the -OH groups stretching vibration peak was shown on the FT-IR spectra of Na-bentonite, SDBS-bentonite and CTAB-bentonite[24,25]. In Fig. 5b, the FT-IR spectra of SDBS-bentonite were no change with Na-bentonite, manifesting SDBS didn't enter into the layers of Na-bentonite. However, new peaks were observed after CTAB inserting into Na-bentonite at 2864 cm^{-1} and 2934 cm^{-1}, which were attributed to stretching vibrations of $-CH_2$ and $-CH_3$ of the aliphatic chain of the surfactant[26]. Furthermore, the FT-IR spectra of CTAB-bentonite displayed $–CH_2$ bending vibration absorption peak in 1480 cm^{-1} (see Fig. 5c) These special peaks proved that surfactant molecules (CTAB) had inserted into between Na-bentonite layers.

Table 1 — Textural properties of samples

Samples	Surface area m^2/g	Pore size nm	Pore volume cm^3/g
a	74.351	3.866	0.137
b	81.680	3.832	0.179
c	32.735	3.865	0.078

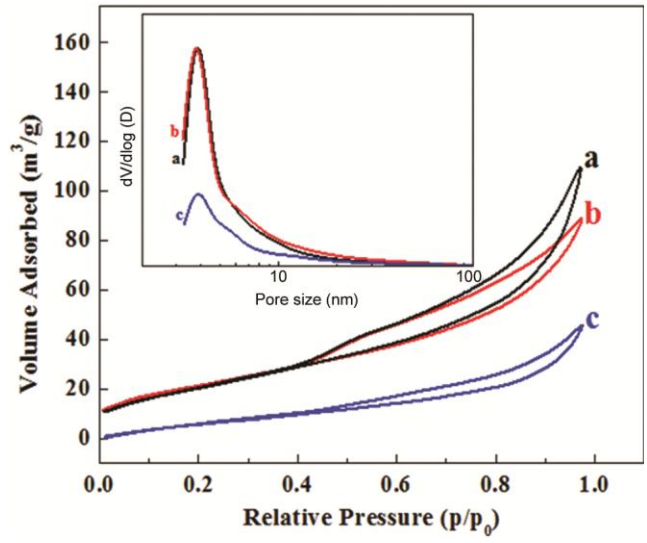

Fig. 4 — N_2 adsorption-desorption isotherms of samples and their corresponding pore size distribution (insert). (a) Na-bentonite, (b) SDBS-bentonite, (c) CTAB-bentonite

Influencing factors for the adsorption performance of modified Na-bentonite

Effect of surface modification and adsorbent the dose on the adsorption of dyes onto organobentonite

Figure 6 displayed the results of adsorbent dosage experiment In Fig. 6, with the dosage of absorbents

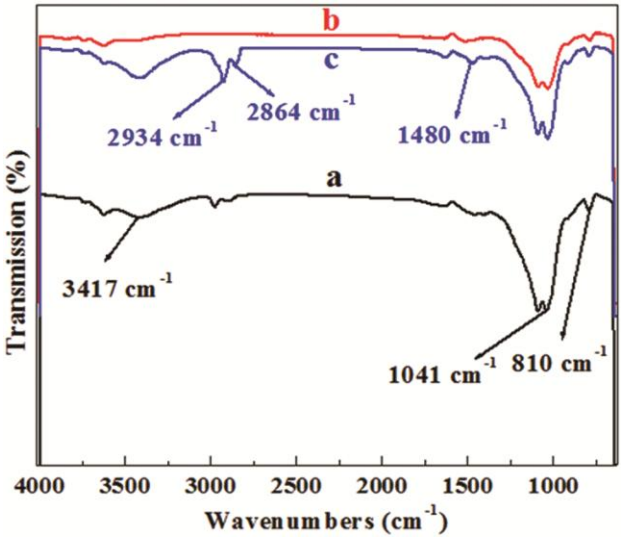

Fig. 5 — FT-IR spectra of samples. (a) Na-bentonite, (b) SDBS-bentonite, (c) CTAB-bentonite

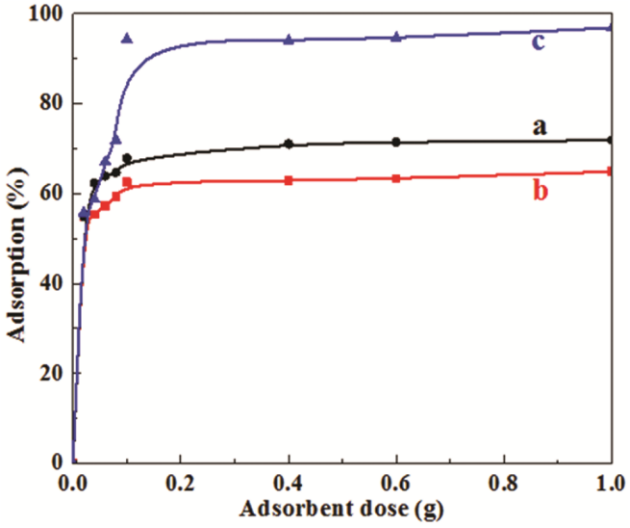

Fig. 6 — Effect of surface modification for the adsorption of RhB onto organobentonite (a) Na-bentonite, (b) SDBS-bentonite, (c) CTAB-bentonite.

increasing, the removal rate of RhB tended to be stable. For Na-bentonite, removal rate reached the maximum (69.06%) in 0.1 g dosing quantity (see Fig.6a). In dose of 0.1 g, the maximum removal rate of adsorption of RhB onto SDBS-bentonite was 64.90% in Fig.6b Obviously, the maximum removal rate of SDBS-bentonite was inferior to the Na-bentonite, which was due to reduce layer spacing of Na-bentonite after SDBS modified bentonite and result in the decrease of its adsorption capacity In Fig.6c, the maximum removal rate of CTAB-bentonite was 94.2%. The value was far more than Na-bentonite and SDBS-bentonite. This suggests the fact that after CTAB inserted Na-bentonite, Na-bentonite layer spacing increased and the hydrophilic surface of Na-bentonite transformed into a hydrophobic surface to improve adsorptive property[27], which was s in conformity with characterization results that CTAB inserted into and SDBS didn't enter the layer of Na-bentonite.

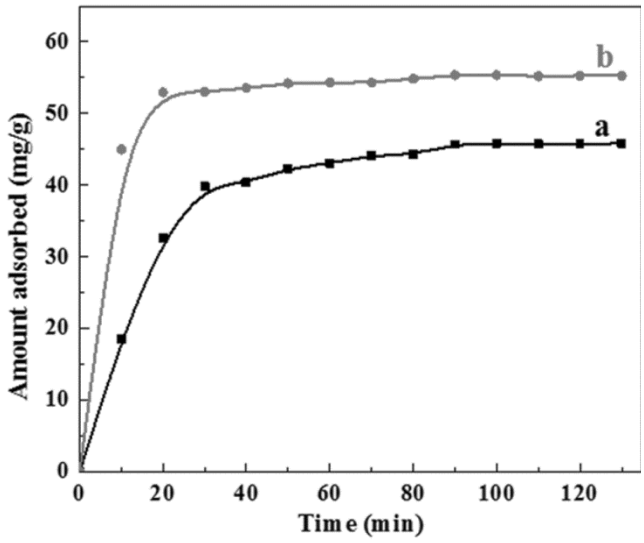

Fig. 7 — Effect of contact time on the adsorption of RhB onto (a) SDBS-bentonite and (b) CTAB-bentonite.

Effect of contact time for adsorption RhB

According to the experimental results of the contact time, plotting adsorption quantity versus time was shown in Fig. 7 From Fig 7, it was obvious that the adsorption amount of RhB onto CTAB-bentonite was much higher than SDBS- bentonite In Fig. 7a, with the increase of contact time, the dye adsorption amount increased slowly and gradually tended to equilibrium for SDBS-bentonite and adsorption process of RhB achieved equilibrium in 90 min, which equilibrium absorption capacity was 45.71 mg/g for RhB As shown in Fig.7b, the equilibrium time was determined to be 40 min for CTAB-bentonite, and the amount adsorbed of RhB was 55.4 mg/g at the initial concentration of 100 mg/L at 30 ^{o}C The high efficiency was due to the abundant availability of adsorption sites on the surface of SBDS-bentonite and CTAB-bentonite at an initial process, but with the increase of adsorption time, adsorption capacity tended to saturate. Therefore, the adsorption time was 90 min as subsequent experiments.

Effect of initial RhB concentrations and temperature

Figure 8 displayed the effect of RhB concentration and temperature on the adsorption by CTAB-bentonite and SDBS-bentonite. In Fig. 8A, amount adsorbed maximum value of RhB were 119.01 mg/g (see Fig. 8A(a)) and 156.20 mg/g (see Fig. 8A(b)) in initial concentration 300 mg/L, respectively. Comparing with Fig 8A (a) and Fig 8A (b), as the initial dyes concentration increased from 50 to 300 mg/L, amount adsorbed increased significantly. And at initial dyes concentration of 300-350 mg/L, adsorption process was a stable state. The results

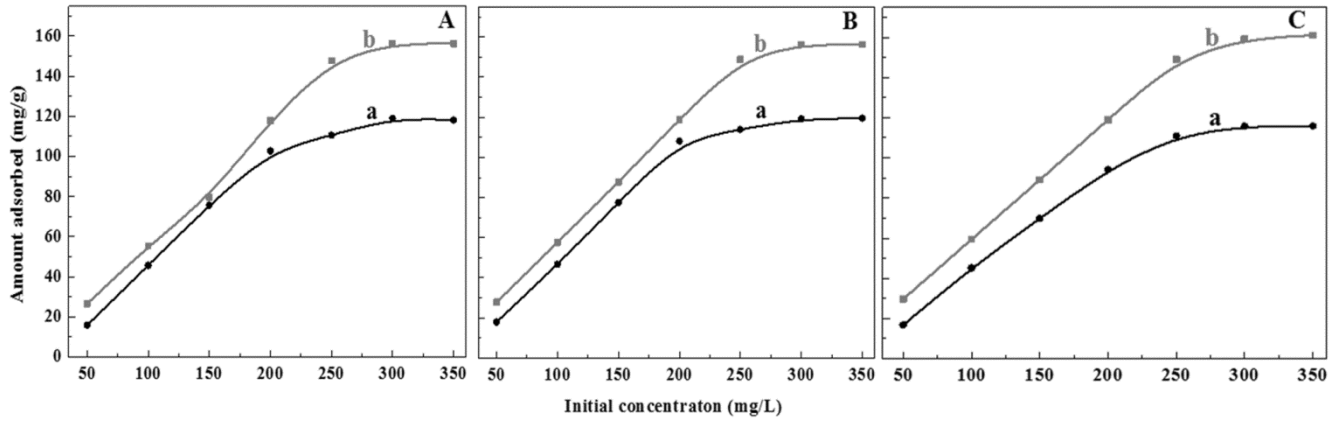

Fig. 8 — Effect of initial concentration and temperature on the adsorption of RhB onto SDBS-bentonite (a) and CTAB-bentonite (b) (A) at 30°C, (B) at 40°C, (C) at 50 ^{o}C

indicated that the initial dye concentration was a significant driving force to overcome all limitations between the aqueous and solid phases[28]. In addition, the maximum adsorption amount of RhB were 119.25 mg/g (see Fig. 8B (a)) and 156.3 mg/g (see Fig. 8B (b)), respectively, which were 115.78 mg/g and 159.10 mg/g at 50°C in Fig. 8C. This proved that the influence of temperature was relatively weak for adsorption of RhB onto SDBS-bentonite and CTAB-bentonite. Therefore, in order to cut down energy consumption, the next experiments condition was initial RhB concentration of 300 mg/L and 30°C solution temperature.

Effect of initial solution pH

The effect of *p*H for adsorption of RhB onto modified bentonite In Fig 9a, it was observed that the optimal adsorption amount of RhB onto SDBS-bentonite was 137.19 mg/g at *p*H of 7.0. With the *p*H increased from 2.0 to 7.0, the adsorption capacity of RhB quickly raised and reduced at *p*H increasing from 2.0 to 9.0, but at *p*H from 9.0 to 10.0, adsorption process of RhB was equilibrium. The adsorption capacity of RhB was aggrandized from 150.21 mg/g to 173.53 mg/g with the solution *p*H increasing from 2.0 to 9.0. However, with *p*H more than 9.0, the adsorption amount almost no longer increased even tended to decrease slowly. Therefore, the optimal *p*H value was 7.0 and 9.0 for SDBS-bentonite and CTAB-bentonite, respectively. Adsorption of dyes onto CTAB-bentonite may take place through ion exchange electrostatic force and partition, which made the adsorption amount to be higher than SDBS modified bentonite[29]. Furthermore, the CTAB surfactant obviously improved lamellar space by close packing of the alkyl chains to create hydrophobic regions, which will create an effective organic environment and promote the adsorbed organic matter[30].

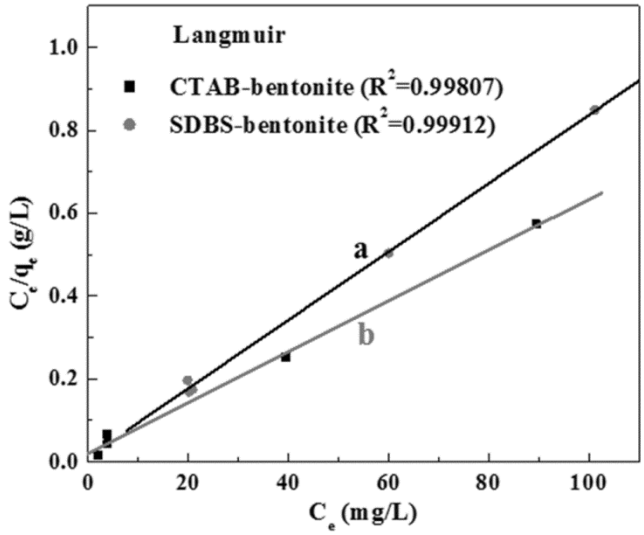

Fig. 9 — The Langmuir adsorption isotherms of RhB onto (a) SDBS-bentonite and (b) CTAB-bentonite.

Adsorption isotherm

The adsorption isotherm was significant for exploring the process of adsorption of RhB onto SDBS-bentonite and CTAB-bentonite. The adsorption date of RhB onto SDBS-bentonite and CTAB-bentonite were applied to fit the models of Freundlich (Eq. (3)) and Langmuir (Eq. (4)). The linear form of the Freundlich and the Langmuir equation were as follows:

$$\ln q_e = \ln K_f + \frac{1}{n}\ln C_e \quad \text{... (3)}$$

$$\frac{C_e}{q_e} = \frac{1}{q_{\max} k_L} + \frac{C_e}{q_{\max}} \quad \text{… (4)}$$

where q_e (mg/g) is the amount of dye adsorbed on the adsorbent at equilibrium, C_e (mg/L) the equilibrium dye concentration in solution, while K_f (L/g) and n are the Freundlich adsorption constants, their value can be obtained by the intercept and slope fitting line of Freundlich model. Where q_{max} (mg/g) is the maximum adsorption amount for the adsorbent and K_L (L/mg) is the Langmuir adsorption constant, their value can be calculated by the intercept and slope fitting line of Langmuir model. While all other symbols of the Langmuir formula are the same as in Eq. (3). The Freundlich equation was applied to describe heterogeneous systems and reversible adsorption and was not confined to the formation of monolayers. However, the Langmuir adsorption isotherm assumed that the adsorption occurs at specific homogenous sites within the adsorbent and was the most suitable for monolayer adsorption Langmuir equilibrium parameter (R_L) was as follow

$$R_L = \frac{1}{\left(1+K_L C_0\right)} \quad \text{… (5)}$$

The value of R_L indicates the type of isotherm either to be unfavorable ($R_L > 1$), linear ($R_L = 1$), favorable ($0 < R_L < 1$) or irreversible ($R_L = 0$).

The fitting results of Langmuir and Freundlich model were displayed on Figure 9 and Figure 10,

respectively. Comparing Fig. 10a and Fig. 10b, we can find that fitting effect of Langmuir model for the adsorption of RhB onto SDBS-bentonite and CTAB-bentonite. The results indicated that SDBS-bentonite had a better fitting effect than CTAB-bentonite. In Table 2, the correlation coefficient (R^2) of SDBS-bentonite and CTAB-bentonite was 0.99912 and 0.99807 in the Langmuir model, respectively, which manifested that it was more suitable to the Langmuir model for SDBS-bentonite adsorption of RhB. In the same way, in Fig. 11a and Fig. 11b, the fitting effect of SDBS-bentonite and CTAB-bentonite were both poorer. The R^2 value of SDBS-bentonite and CTAB-bentonite were respectively 0.72279 and 0.69496 from Table 2 In addition, from Table 2, the R_L values were 0.0033 and 0.0427 respectively. They belonged to the favorable limits. Therefore, the Langmuir model was more appropriate for adsorption of RhB onto SDBS-bentonite and CTAB-bentonite.

Adsorption kinetics

Adsorption test data of RhB onto modified bentonite carried out dynamic study and analyzed their adsorption mechanism. The frequently-used dynamic model includes pseudo-first-order and pseudo-second-order model. The pseudo-first-order kinetics adsorption model was invariably described for the adsorption of solid/liquid systems[31]. The pseudo-second-order model may be chemical adsorption, which concerns valence forces by sharing or electron exchange action[32]. The pseudo-first-order (Eq (6)) and pseudo-second-order (Eq (7)) kinetics model were as follows:

$$\ln(q_e - q_t) = \ln q_e - tK_1 \quad \ldots (6)$$

$$\frac{t}{q_t} = \frac{1}{q_e^2 K_2} + \frac{t}{q_e} \quad \ldots (7)$$

where K_1 (min^{-1}) and K_2 ($g\cdot mg^{-1}min^{-1}$) are respectively pseudo-first-order and pseudo-second-order adsorption rate constant, q_e and q_t are the adsorption loading of RhB (mg/g) at equilibrium and at time t (min), respectively. For the pseudo-first-order kinetics, plotting $\ln(q_e - q_t)$ versus t (Fig. 11) should provide a straight line and K_1 can be determined from

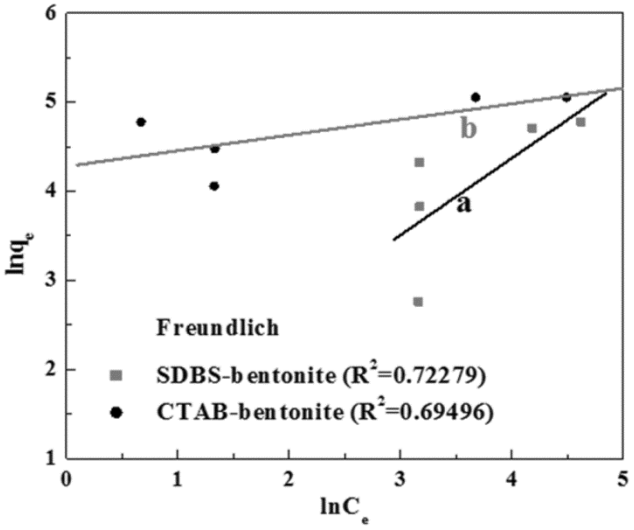

Fig. 10 — The Freundlich adsorption isotherms of RhB onto (a) SDBS-bentonite and (b) CTAB-bentonite.

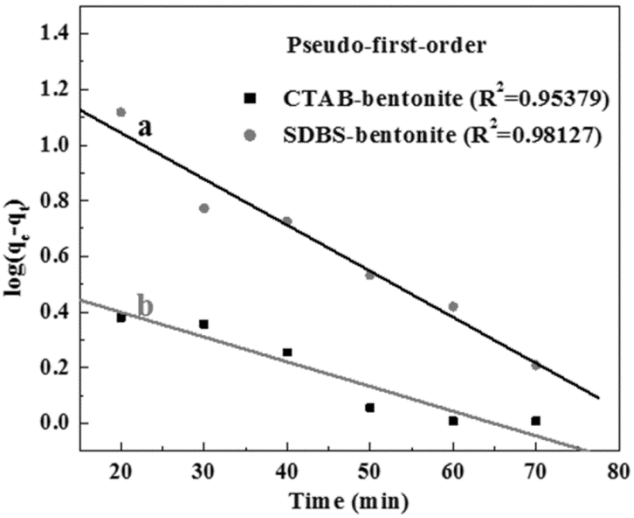

Fig. 11 — The pseudo-first-order kinetic for the adsorption of RhB onto SDBS-bentonite (a) and CTAB-bentonite (b).

Table 2 — Isotherm parameters analysis coefficient for the adsorption of RhB onto SDBS-bentonite and CTAB-bentonite

Isotherm	Parameters	SDBS-bentonite	CTAB-bentonite
Langmuir	q_{max} (mg/g)	120.9819	156.3169
	K_L (L/mg)	0.8689	0.0641
	R^2	0.99912	0.99807
	R_L	0.0033	0.0427
Freundlich	K_f (L/g)	4.1569	72.1278
	N	1.3151	5.6951
	R^2	0.72279	0.69496

the slope. For the pseudo-second-order kinetics, plotting t/q_t against t (Fig. 12), a straight line was obtained and the rate constant K_2 can be calculated according to the straight line of intercept. All the parameters of the calculation results were presented in Table 3.

From Table 3, the R^2 values of pseudo-first-order and pseudo-second-order were 0.98127 and 0.99868 for adsorption of RhB onto SDBS-bentonite, which indicated that the pseudo-second-order dynamic model was more suitable for describing SDBS-bentonite adsorption of RhB. For CTAB-bentonite, the R^2 values were 0.95379 and 0.99996 for pseudo-first-order and pseudo-second-order. Compared with SDBS-bentonite, the R^2 values of the pseudo-second-order was higher for CTAB-bentonite. To sum up, the pseudo-second-order dynamic model was more accurate to portray adsorption of RhB onto modified bentonite.

Thermodynamic study

Thermodynamic parameters such as standard free energy change (ΔGº), standard entropy change (ΔSº) and standard enthalpy change (ΔHº) can be gained by the following equations:

$$K_c = \frac{q_e}{C_e} \quad \ldots (8)$$

$$\Delta G^o = -RT \ln K_c \quad \ldots (9)$$

$$\Delta G^o = \Delta H^o - T\Delta S^o \quad \ldots (10)$$

$$\ln K_c = -\frac{\Delta G^o}{RT} = \frac{\Delta S^o}{R} - \frac{\Delta H^o}{RT} \quad \ldots (11)$$

where K_c is the equilibrium constant The values of ΔHº and ΔSº were calculated by slope and intercept of plotting $\ln K_c$ against 1/T (Fig. 13) Table 4

Table 3 — Kinetic models parameters obtained in adsorption of RhB onto SDBS-bentonite and CTAB-bentonite

Kinetic models	Parameters	SDBS-bentonite	CTAB-bentonite
Pseudo-first-order	q_e (mg/g)	39.5429	52.4636
	K_1 (min^{-1})	0.0166	0.1570
	R^2	0.98127	0.95379
Pseudo-second-order	q_e (mg/g)	46.5639	55.4723
	K_2 (g• $mg^{-1}min^{-1}$)	0.0024	0.0199
	R^2	0.99868	0.99996

Table 4 — Thermodynamic parameters for the adsorption of RhB by organobentonite.

T	CTAB-bentonite			SDBS-bentonite		
(K)	ΔHº (kJ/mol)	ΔSº(J/k mol)	ΔGº(kJ/mol)	ΔHº(kJ/mol)	ΔSº(J/k mol)	ΔGº(kJ/mol)
303			-3.4430			-2.8323
313	6.0966	31.4839	-3.7579	3.2254	9.3583	-2.9259
323			-4.0727			-3.0195

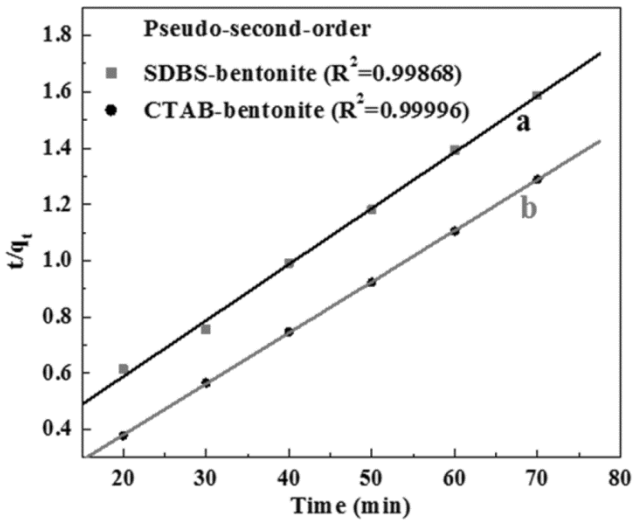

Fig. 12 — The pseudo-second-order kinetic for the adsorption of RhB onto SDBS-bentonite (a) and CTAB-bentonite (b).

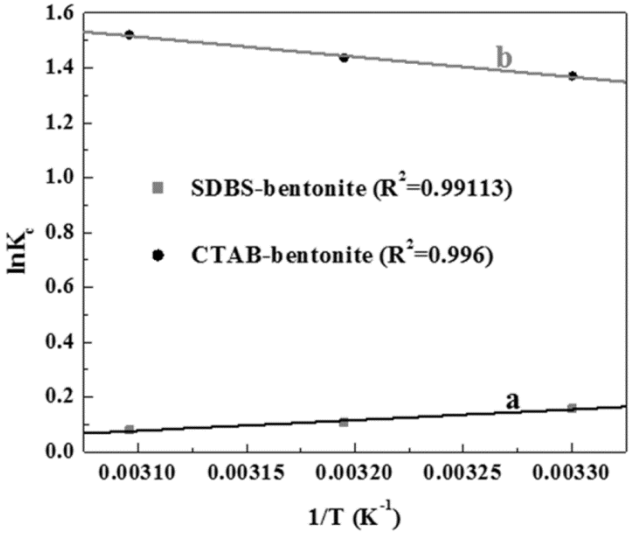

Fig. 13 — Plots of $\ln K_c$ versus 1/T for RhB onto (a) SDBS-bentonite and (b) CTAB-bentonite.

summarizes the thermodynamic parameters at different temperatures for the adsorption of RhB onto CTAB-bentonite and SDBS-bentonite.

In Table 4, the ΔS^o and ΔH^o of two kinds of adsorbent were both positive values, which manifested that adsorption of RhB onto SDBS-bentonite and CTAB-bentonite was an endothermic process and random And some structural change took place among the active sites of the adsorbent and the dye[33]. Moreover, the ΔG^o values of SDBS-bentonite and CTAB-bentonite were less than zero at different temperatures. The negative values of ΔG^o shown that adsorption process was spontaneous and feasible for the modified bentonite.

Conclusion

The study investigated the structure characterization and adsorption property of anionic (SDBS) and cationic (CTAB) surfactant modified sodium bentonite. The results show that anionic (SDBS) modified led to reduce surface area and layer spacing of sodium bentonite and decrease the adsorption capacity, by contrast, cationic modification of sodium bentonite layer spacing increased and the adsorption performance is greatly improved. The maximum adsorption amount of RhB is 173.5 mg/g (*p*H=9 0) onto CTAB-bentonite and 137.19 mg/g (*p*H=7.0) onto SDBS- bentonite, respectively. The adsorption of RhB onto surfactant modified Na-bentonite equilibrate within 90 min. At the same time, the adsorption kinetics of RhB onto the modified bentonite samples can be accurately described by the pseudo-second-order model and that the adsorption isotherm was in good conformity with the Langmuir equation. Thermodynamic studies reveal that the adsorption process of RhB was spontaneous and exothermic. The modification of bentonite with cationic surfactant is an economical and feasible method to enhance its adsorption properties.

Acknowledgement

This work was supported by the National Natural Science Foundation of China (21676028), the Natural Science Foundation of Shanxi(201901D111068) China Postdoctoral Science Foundation Funded Project (2019M651083) and the Shanxi Provincial Key Research and Development Plan (general) Social Development Project(201703D321009-5).

References

1 Santos S C R, Oliveira A F M & Boaventura R A R, *J Cleaner Prod*, 126 (2016) 667.
2 Zhang L J, Hu P, Wang J & Huang R H, *Appl Surf Sci*, 369 (2016) 558.
3 Sarma G K, Gupta S S & Bhattacharyya K G, *J Environ Manag*, 171 (2016) 1.
4 Soltani R D C, Jorfi S, Safari M & Rajaei M S, *J Environ Manag*, 179 (2016) 47.
5 Wang C J, Jiang X H, Zhou L M, Xia G Q, Chen Z J, Duan M & Jiang X M, *Chem Engin J*, 219 (2013) 469.
6 Hassani A, Vafaei F, Karaca S & Khataee A R, *J Ind Eng Chem*, 20 (2014) 2615.
7 Ranđelović M S, Purenović M M, Matović B Z, Zarubica A R, Momččilović M Z & Purenović J M, *Microp Mesop Mater*, 195 (2014) 67.
8 Amin M T, Alazba A A & Shafiq M, *Sustainability*, 7 (2015) 15302.
9 Latif A, Noor S, Sharif Q M & Najeebullah M, *J Chem Soc Pak*, 32 (2010) 115.
10 Holkar C R, Jadhav A J, Pinjari D V, Mahamuni N M & Pandit A B, *J Environ Manag*, 182 (2016) 351.
11 Miralles-Cuevas S, Oller I, Agüera A, Pérez J A S, Ricardo S M, Malato S, *Environ Sci Water Res Technol*, 2 (2016) 511.
12 Kanagaraj J,Senthilvelan T & Panda R C, *Clean Technol Environ Policy*, 17 (2015) 1443.
13 Türgaya O, Ersöza G, Atalaya S & Forssb J, *Sep Purif Technol*, 79 (2011) 26.
14 Qi L Q, Wang X J & Xu Q K, *Desalination*, 270 (2011) 264.
15 Parolo M E, Pettinari G R & Musso T B, *Appl Surf Sci*, 320 (2014) 356.
16 Yan L G, Qin L L & Yu H Q, *J Mol Liq*, 211 (2015) 1074.
17 Wang E W, Hu L & Lei S M, *Appl Clay Sci*, 118 (2015) 138.
18 Toor M, Jin B & Dai S, *J Ind Engin Chem*, 21 (2015) 653.
19 Orucoglu E & Schroeder P A, *Appl Clay Sci*, 132 (2016) 90.
20 Kotal M & Bhowmick A K, *Prog Poly Sci*, 51 (2015) 127.
21 Xi Y F, Frost R & He H P, *J Colloid Interf Sci*, 305 (2007) 150.
22 Li S Z & Wu P X, J *Hazard Mate*, 173 (2010) 62.
23 Mohammed M I & Baytak S, *Arab J Sci Eng*, 41 (2016) 4775.
24 Chen D M, Chen J & Luan X L, *Chem Engin J*, 171 (2011) 1150.
25 Li Y M, Bi M L, Wang Z P, Li R, Shi K L & Wu W S, J *Taiwan Inst Chem Eng*, 62 (2016) 104.
26 Schampera B, Šolc R, Tunega D & Dultz S, *Appl Clay Sci*, 120 (2016) 91.
27 Sun J L, Zhuang G Z & Wu S Q, *RSC Adv*, 6 (2016) 54747.
28 Lin K L, Pan J Y, Chen Y W, Cheng R M & Xu X C, *J Hazard Mater*, 161 (2009) 231.
29 Zhao F P, Repo E, Yin D L, Meng Y, Jafari S L & Sillanpa M, *Environ Sci Technol*, 49 (2015) 10570.
30 Chinoune K, Bentaleb K, Bouberka Z & Nadimb A, *Appl Clay Sci*, 123 (2016) 64.
31 Zaghouane-Boudiaf H, Boutahala M, Sahnoun S, Tiar C & Gomri F, *Appl Clay Sci*, 90 (2014) 81.
32 Toor M & Jin B, *Chem Eng J*, 187 (2012) 79.
33 Abbasa M & Trari M, *Proc Safety Environ Protect*, 98 (2015) 424.